J. Fluid Mech. (1980), *vol.* 98, *part* 2, *pp.* 273–284
Printed in Great Britain

Linear stability of Poiseuille flow in a circular pipe

By HAROLD SALWEN, FREDRICK W. COTTON

Department of Physics and Engineering Physics, Stevens Institute of Technology, Hoboken, New Jersey 07030

AND CHESTER E. GROSCH

Department of Oceanography and Department of Mathematics, Old Dominion University, Norfolk, Virginia 23508

(Received 16 August 1979)

Correction of an error in the matrix elements used by Salwen & Grosch (1972) has brought the results of the matrix-eigenvalue calculation of the linear stability of Hagen–Poiseuille flow into complete agreement with the numerical integration results of Lessen, Sadler & Liu (1968) for azimuthal index $n = 1$. The $n = 0$ results were unaffected by the error and the effect of the error for $n > 1$ is smaller than for $n = 1$. The new calculations confirm the conclusion that the flow is stable to infinitesimal disturbances.

Further calculations have led to the discovery of a degeneracy at Reynolds number $R = 61{\cdot}452 \pm 0{\cdot}003$ and wavenumber $\alpha = 0{\cdot}9874 \pm 0{\cdot}0001$, where the second and third eigenmodes have equal complex wave speeds. The variation of wave speed for these two modes has been studied in the vicinity of the degeneracy and shows similarities to the behaviour near the degeneracies found by Cotton and Salwen (see Cotton 1977) for rotating Hagen–Poiseuille flow. Finally, new results are given for $n = 10$ and 30; the $n = 1$ results are extended to $R = 10^6$; and new results are presented for the variation of the wave speed with αR at high Reynolds number. The high-R results confirm both Burridge & Drazin's (1969) slow-mode approximation and more recent fast-mode results of Burridge.

In 1972, two of us published the results of a matrix-eigenvalue calculation (Salwen & Grosch 1972; hereinafter referred to as SG) of the linear stability of Poiseuille flow in a circular pipe to both axisymmetric and non-axisymmetric disturbances. That paper was one of a number of papers (see SG for references) which led to the conclusion that Hagen–Poiseuille flow is stable to infinitesimal disturbances. There was, however, some doubt about the accuracy of the numerical results because of differences of up to 30 % between SG and the numerical integration of Lessen, Sadler & Liu (1968; hereinafter referred to as LSL).

In the course of extending the techniques of SG to more general problems, we had occasion to re-do some of the calculations and we discovered a sign error in one term of the matrix elements, the correction of which eliminated the disagreement with LSL (Cotton, Salwen & Grosch 1975; Cotton 1977). We report here on those corrections as well as on newer calculations with the corrected matrix.

The method of calculation has been described in SG. Most of the results reported here were obtained with a new program, designed to be extendable to an annular

0022-1120/80/4444-8970 $02.00

geometry, in which the matrices are obtained in double precision (19 significant figures) and the eigenvalues are calculated in single precision (8 significant figures) on the DEC system-10. Use of a new double-precision Bessel function routine (Cotton & Salwen 1976) has extended the range to $0 \leqslant n \leqslant 30$. Some of the eigenvalues have been calculated in double precision as a test of round-off error and many have been calculated for various matrix sizes as a test of truncation error. Numerous checks against the (corrected) single-precision routine of SG have also been run. Since the two programs start with formulae which, though mathematically equivalent, are considerably different in form, agreement between their results is a check against programming error as well as round-off error. (It was the initial disagreement between these programs which led to the discovery of the error in SG.)

The error in the SG program occurred only for $n \neq 0$; therefore, the $n = 0$ results in SG need no correction. For $n = 1$, we present, in table 1, a comparison between complex wave speeds calculated by LSL†, by the uncorrected SG program, and by the corrected program (labelled CSG).‡ Except for a $\frac{1}{2}$ % difference in mode 3 at $R = 100$ (which we believe to be a misprint in the LSL results), our new results agree with those of LSL to four or five significant figures. In figure 1, we show the corrected wave speeds for $n = 1$, $\alpha = 1$, $10 \leqslant R \leqslant 10^6$. To extend the earlier results to $R = 10^6$, we used a maximum matrix size of 200×200.

In figure 1, modes 2 and 3 appear to be degenerate at $R \sim 61$, since the real and imaginary parts, $c_{\mathscr{R}}$ and $c_{\mathscr{I}}$ of c both appear to be equal for the two modes. A detailed study of the data reveals, however, that the $c_{\mathscr{R}}$ curves for the two modes cross but the $c_{\mathscr{I}}$ curves approach each other closely and then move apart; for this reason, we pointed out in SG that this was *not* a degeneracy. The recent discovery (Cotton 1977) of degeneracies in the eigenvalues for rotating Poiseuille flow has led us to investigate this point more closely.

Figure 2 shows expanded plots of $c_{\mathscr{R}}$ and $c_{\mathscr{I}}$ *vs.* αR for the two nearly-degenerate modes, at $\alpha = 1{\cdot}00$ and $0{\cdot}97$, in the range $57 \leqslant \alpha R \leqslant 63$. For $\alpha = 1{\cdot}00$ the modes are labelled 2 and 3; for $\alpha = 0{\cdot}97$, they are labelled 2′ and 3′. It is clear from this figure that, at $\alpha = 1{\cdot}00$, the real parts cross but not the imaginary parts while, at $\alpha = 0{\cdot}97$, the imaginary parts cross but not the real parts. Apart from this crossing behaviour (which makes it impossible to uniquely order the modes without destroying the continuity of c as a function of α), the eigenvalues are quite similar at the two values of α.

At each α between 0·97 and 1, there is a value of R at which either $c_{\mathscr{R}}$ or $c_{\mathscr{I}}$ is the same for the two modes. For *one* value of α in the range (simultaneously the highest for which $c_{\mathscr{I}}$ is the same and the lowest for which $c_{\mathscr{R}}$ is the same), there is a value of R for which $c_{\mathscr{R}}$ and $c_{\mathscr{I}}$ are both the same; i.e. the two modes have the same complex wave speed $c_2 = c_3$.

In figure 3, we have plotted the curves for $c_{2\mathscr{R}} = c_{3\mathscr{R}}$ and $c_{2\mathscr{I}} = c_{3\mathscr{I}}$ in the α, (αR) plane. They appear to be two parts of a single smooth curve, joining at the point of degeneracy where $c_2 = c_3$. The degeneracy occurs at $\alpha = 0{\cdot}9874 \pm 0{\cdot}0001$, $\alpha R = 60{\cdot}678 \pm 0{\cdot}001$ ($R \sim 61{\cdot}452$). As $\alpha \rightarrow 0$, $\alpha R \rightarrow \sim 63{\cdot}6$ along the $c_{2\mathscr{I}} = c_{3\mathscr{I}}$ curve and, as $\alpha R \rightarrow 0$, $\alpha \rightarrow \sim 2{\cdot}5$ along the $c_{2\mathscr{R}} = c_{3\mathscr{R}}$ curve.

† We again thank these authors for their numerical results which they sent us when we were preparing the figures of SG.

‡ The complex wave speed c, is defined by the assumed form $e^{i\alpha(z-ct)+in\theta}$ for the disturbances.

R	MODE 1		MODE 2		MODE 3		MODE 4		
100	0·54835	0·15782	0·55089	0·36044	0·78718	0·48330	0·66069	0·74845	SG
	0·57256	0·14714	0·55198	0·37446	0·78735	0·47946	0·66247	0·74907	CSG
	0·57256	0·14713	0·55198	0·37446	0·78250	0·47946	0·66247	0·74907	LSL
160	0·61469	0·15706	0·50007	0·20143	0·81672	0·37765	0·60260	0·45140	SG
	0·61801	0·13141	0·52113	0·22954	0·81713	0·37479	0·60381	0·45334	CSG
	0·61799	0·13141	0·52136	0·22946	0·81712	0·37483	0·60380	0·45334	LSL
200	0·64956	0·14753	0·48195	0·17881	0·83394	0·33925	0·57535	0·34003	SG
	0·64527	0·12921	0·51116	0·20266	0·83430	0·33702	0·57487	0·33814	CSG
	0·64526	0·12920	0·51117	0·20265	0·83429	0·33703	0·57486	0·33813	LSL
240	0·67946	0·14411	0·47256	0·17355	0·84789	0·31097	0·55430	0·26181	SG
	0·67138	0·13231	0·50843	0·21034	0·84825	0·30920	0·55013	0·23976	CSG
	0·67138	0·13231	0·50844	0·21033	0·84824	0·30920	0·55011	0·23976	LSL
300	0·71888	0·13396	0·45212	0·17860	0·86439	0·27924	0·53878	0·12939	SG
	0·71295	0·12900	0·45788	0·21300	0·86478	0·27793	0·56173	0·16498	CSG
	0·71286	0·12907	0·45789	0·21300	0·86478	0·27793	0·56171	0·16497	LSL
600	0·80470	0·09267	0·36680	0·17004	0·90545	0·19749	0·48810	0·11884	SG
	0·80258	0·09101	0·36518	0·18222	0·90587	0·19697	0·51585	0·11474	CSG
	—	—	0·36519	0·18222	—	—	0·51583	0·11472	LSL
1000	0·84809	0·07152	0·31064	0·15347	0·92698	0·15296	0·44668	0·08558	SG
	0·84675	0·07086	0·30947	0·15973	0·92730	0·15270	0·46916	0·09117	CSG
	0·84675	0·07086	—	—	0·92730	0·15270	0·46924	0·09090	LSL
3000	0·91187	0·04132	0·21715	0·11518	0·95806	0·08838	0·36189	0·04784	SG
	0·91147	0·04127	0·21679	0·11688	0·95821	0·08835	0·37095	0·06168	CSG
	0·91147	0·04129	—	—	—	—	0·371	0·0616	LSL
6000	0·93756	0·02926	0·17316	0·09409	0·97041	0·06253	0·31205	0·03909	SG
	0·93738	0·02927	0·17299	0·09486	0·97049	0·06253	0·31332	0·05216	CSG
	0·93737	0·02926	—	—	—	—	0·313	0·0521	LSL
9600	0·95059	0·02315	0·14846	0·08164	0·97663	0·04945	0·27946	0·03712	SG
	0·95048	0·02317	0·14836	0·08209	0·97668	0·04946	0·27681	0·04760	CSG
	—	—	—	—	—	—	0·277	0·0476	LSL

TABLE 1. Calculated complex wave speeds, for $n = 1$, $\alpha = 1$, obtained with uncorrected matrix (SG), corrected matrix (CSG) and numerical integration (LSL). All of the imaginary parts are negative, but the negative signs have been omitted for clarity.

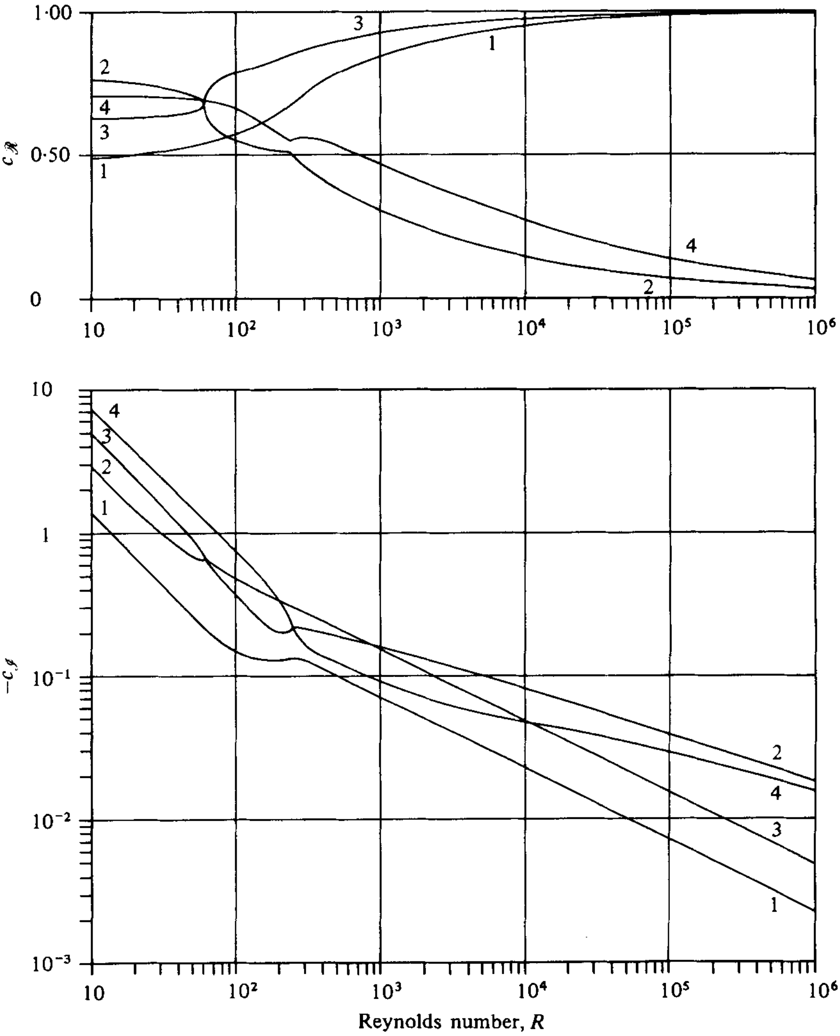

FIGURE 1. Real and imaginary parts of the complex wave speed, c, as a function of the Reynolds number, R, for $n = 1$, $\alpha = 1{\cdot}00$. The modes shown are the four least stable modes as $R \rightarrow 0$. At $R = 10^6$, they are the 1st, 19th, 2nd and 15th modes respectively.

At the point of degeneracy, there can, in principle, be either two linearly independent eigenfunctions corresponding to the same eigenvalue or one eigenfunction and one generalized eigenfunction (see, e.g. Di Prima & Habetler 1969). We cannot investigate this directly, because our calculation yields a numerical estimate of the point of degeneracy – not the exact value. At any point we choose, the eigenvalues will not be identical, so there must be two different eigenvectors. To determine whether there are two eigenvectors at the point of degeneracy, we studied the behaviour of

$$\cos\theta_{23} = \frac{|(v_2, v_3)|}{[(v_2, v_2)\,(v_3, v_3)]^{\frac{1}{2}}}, \tag{1}$$

the cosine of the 'angle' between the numerical eigenvectors, for (α, R) near the point

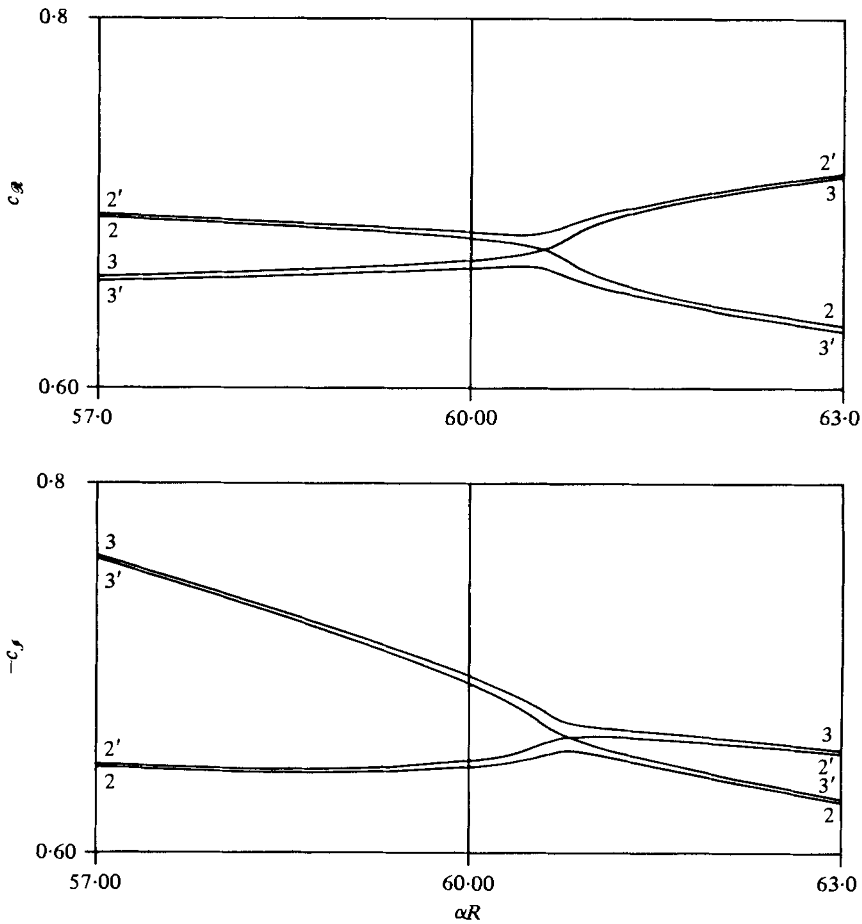

FIGURE 2. Real and imaginary parts of the complex wave speed, c, as a function of αR for $n = 1$, $\alpha = 1{\cdot}00$ and $0{\cdot}97$. The modes shown are the 2nd and 3rd least stable modes as $R \to 0$. They are labelled $(2, 3)$ for $\alpha = 1{\cdot}00$ and $(2', 3')$ for $\alpha = 0{\cdot}97$.

of degeneracy. As (α, R) gets closer to the point of degeneracy, our values for $\cos\theta_{23}$ get closer to 1, reaching 0·999998 at the closest point. This indicates that the two eigenvectors approach each other as (α, R) approaches the point of degeneracy, so that there is one eigenvector and one generalized eigenvector corresponding to the degenerate eigenvalue.

As examples of results for higher n, we present, in figures 4 and 5, the variation of c with R for five and four modes, respectively, at $n = 10$ and 30, $\alpha = 1$. Figure 4, for $n = 10$, shows similar features to figure 1 – many crossings, a near degeneracy between modes 4 and 5 at $R \sim 1380$, and a division into 'fast' and 'slow' modes (with $c \to 1$ and 0 respectively) for high R – but the change-over from low- to high-R behaviour takes place at a somewhat higher Reynolds number. Figure 5 is much simpler, at least partly because all the modes plotted (the four least-stable modes as $R \to 0$) are slow modes at high R.

Extension of our calculations to higher Reynolds numbers (by means of larger matrices) has made possible a further study of the high R behaviour of the eigenvalues

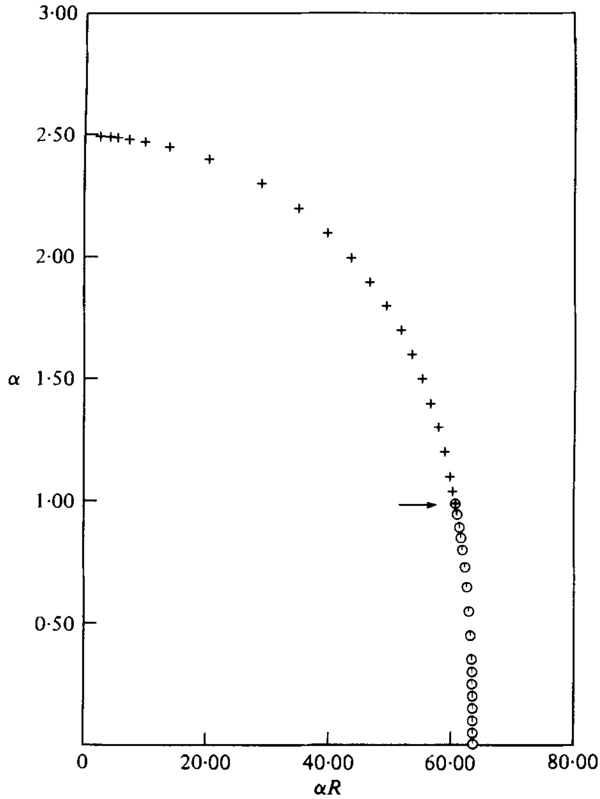

FIGURE 3. The curves $c_{2\mathscr{R}} = c_{3\mathscr{R}}$ and $c_{2\mathscr{I}} = c_{3\mathscr{I}}$ in the α, (αR) plane. ⊖, $c_{2\mathscr{I}} = c_{3\mathscr{I}}$; +, $c_{2\mathscr{R}} = c_{3\mathscr{R}}$; ⊕, $c_2 = c_3$, degeneracy. The arrow points to the location of the degeneracy at $\alpha = 0{\cdot}9874 \pm 0{\cdot}0001$, $\alpha R = 60{\cdot}678 \pm 0{\cdot}0001$ $(R \sim 61{\cdot}452)$. The error in the location of each computed point is at least two orders of magnitude less than the size of the symbols.

for the 'fast' and 'slow' eigenmodes. As in SG, we have tried to fit our results to the forms given by Burridge & Drazin (1969),

$$c = 1 - \lambda/(\alpha R)^{\frac{1}{2}}, \tag{2}$$

for 'fast' modes and

$$c = \mu/(\alpha R)^{\frac{1}{3}}, \tag{3}$$

for 'slow' modes.

In the case of the fast modes, we were able to fit our high-R, low-α results to (2) for a number of modes, with λ essentially constant for $\alpha R \gtrsim 10^5$, $\alpha \lesssim 0{\cdot}1$ and approximately constant for $\alpha R \gtrsim 10^4$, $\alpha \lesssim 1$. Table 2 lists the values of λ obtained for $1 \leqslant n \leqslant 9$ and figure 6 shows the location in the complex plane of these coefficients for $1 \leqslant n \leqslant 6$. Our calculated results occur in pairs which are symmetrical about the line arg $(\lambda) = \frac{1}{4}\pi$ and lie approximately on two lines nearly parallel to it. Burridge & Drazin no longer claim that the approximation used in their paper is valid for these low-lying modes. Instead, Burridge has carried out a new calculation of the coefficient, λ, for the least stable mode for $1 \leqslant n \leqslant 10$.† Burridge's results for $n \leqslant 9$ are included in table 2 and are in good agreement with our results for $n \leqslant 7$.

† D. M. Burridge & P. G. Drazin, private communication.

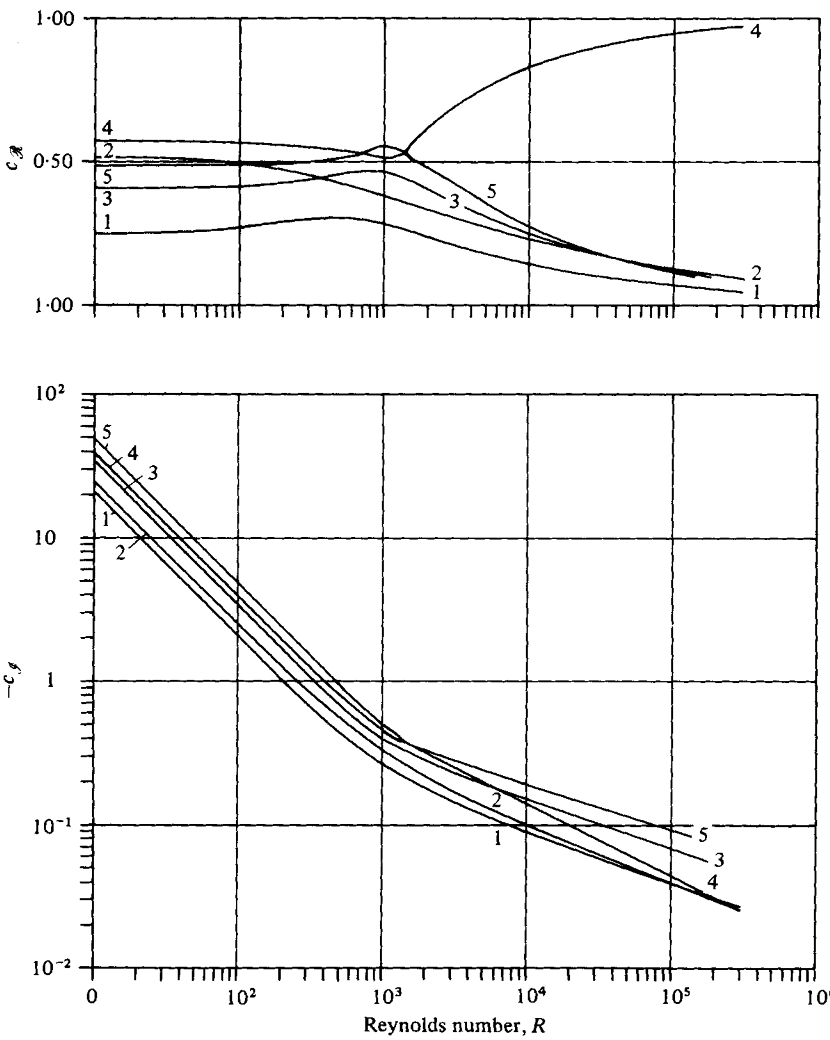

FIGURE 4. Real and imaginary parts of the complex wave speed, c, as a function of the Reynolds number, R, for $n = 10$, $\alpha = 1{\cdot}00$. The modes shown are the five least stable modes as $R \to 0$.

For the slow modes, our values of $(\alpha R)^{\frac{1}{3}}c$ are not constant, but vary slowly with αR, presumably because we have not reached sufficiently high values of αR. We therefore fit our wave speeds for $\alpha R = 5 \times 10^4$, 1×10^5 and 2×10^5, $0 \leqslant n \leqslant 9$ to the form

$$c = \mu/(\alpha R)^{\frac{1}{3}} + \mu_1/(\alpha R)^{\frac{2}{3}} + \mu_2/(\alpha R) \tag{4}$$

in order to obtain an extrapolation to the value of μ as $\alpha R \to \infty$. Some of our results are presented in table 3, along with coefficients calculated from the formulae of Burridge & Drazin. The remarkable agreement with their n-independent theory is characteristic of all of our results for μ.

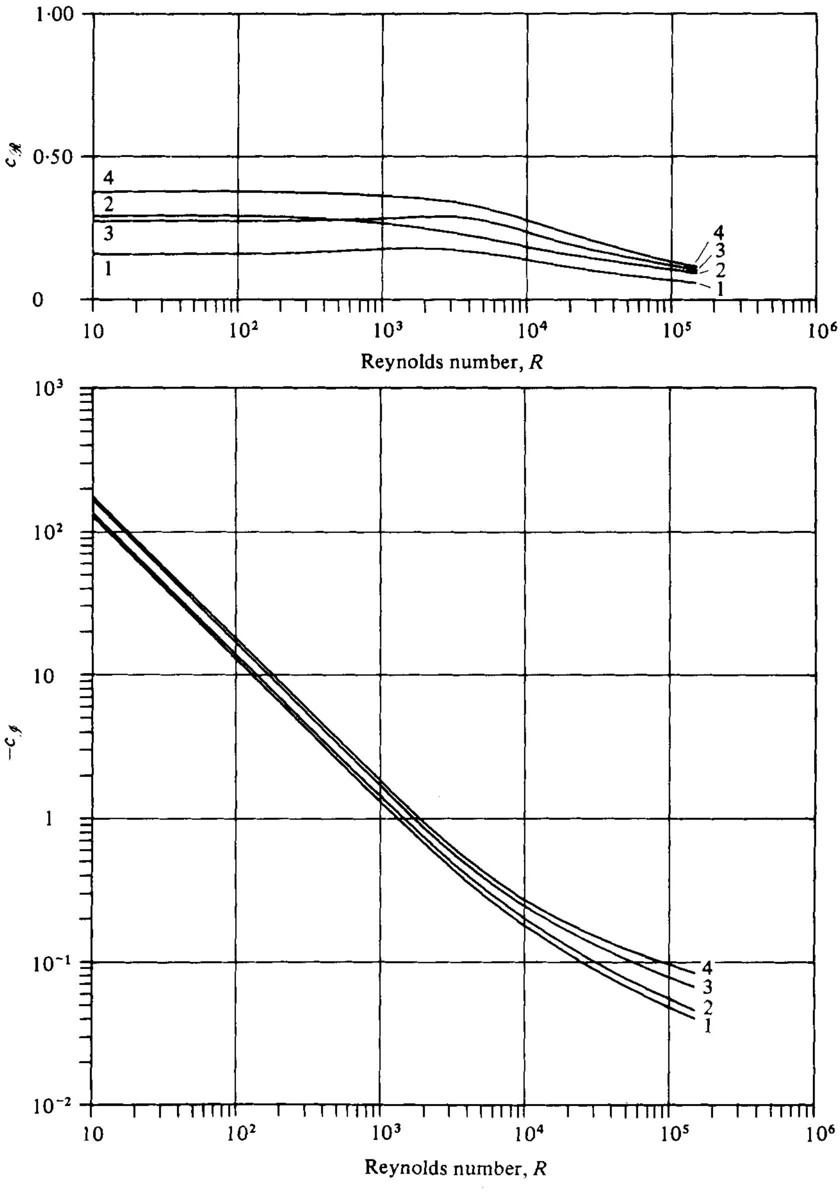

FIGURE 5. Real and imaginary parts of the complex wave speed as a function of the Reynolds number, R, for $n = 30$, $\alpha = 1{\cdot}00$. The modes shown are the four least stable modes as $R \to 0$.

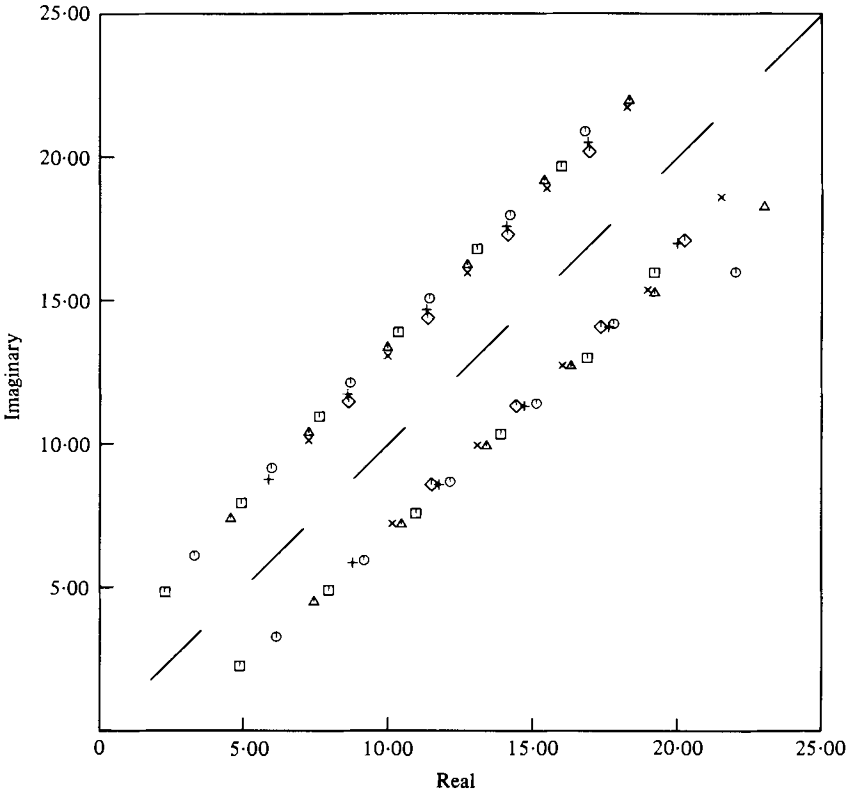

FIGURE 6. A plot of the numerical results for the coefficient λ in equation (2) (fast mode approximation) for $1 \leqslant n \leqslant 6$. The numerical results fall along two nearly-parallel lines, symmetrical about the dashed line, $\lambda_{\mathscr{R}} = \lambda_{\mathscr{I}}$. The n values are: □, 1; ⦶, 2; △, 3; +, 4; ×, 5; ◇, 6. Each of the roots along one line is paired with a root along the other line. Note that the error in the numerical results increases with increasing $|\lambda|$ (see table 2).

n	1st pair		2nd pair		3rd pair		4th pair		5th pair		6th pair	
1	4·8550	2·28055	7·9491	4·9200	10·949	7·615	13·89	10·354	16·9	13·0	19·2	16
	(4·855	2·281)										
	2·28054	4·85510	4·9198	7·9488	7·617	10·949	10·348	13·905	13·07	16·82	16·0	19·7
2	6·1316	3·3001	9·1691	5·973	12·143	8·683	15·12	11·42	17·8	14·2	22	16
	(6·131	3·301)										
	3·3002	6·1316	5·9724	9·1690	8·685	12·1415	11·42	15·08	14·2	18·0	16·8	20·9
3	7·4405	4·5499	10·437	7·2480	13·384	9·968	16·31	12·75	19·2	15·3	23	18·3
	(7·438	4·552)										
	4·5499	7·4407	7·2468	10·4349	9·974	13·390	12·73	16·31	15·4	19·2	18·3	22·0
4	8·7837	5·8798	11·748	8·597	14·681	11·325	17·65	14·09	20·0	17·0		
	(8·772	5·844)										
	5·8799	8·7835	8·596	11·748	11·334	14·687	14·08	17·59	16·9	20·5		
5	10·1481	7·241	13·090	9·977	16·02	12·723	18·95	15·4	21·53	18·6		
	(10·12	7·255)										
	7·243	10·1483	9·976	13·091	12·721	16·014	15·48	18·93	18·26	21·81		
6	11·5270	8·6268	14·449	11·368	17·38	14·10	20·22	17·1				
	(11·50	8·680)										
	8·6261	11·5261	11·370	14·455	14·11	17·369	16·93	20·23				
7	12·9132	10·0180	15·827	12·772	18·79	15·50	21·0	18·3				
	(13·03	10·30)										
	10·0182	12·9134	12·770	15·829	15·51	18·73	18·4	21·7				
8	14·306	11·415	17·20	14·18	20·2	16·94						
	(15·68	11·16)										
	11·416	14·307	14·17	17·21	16·92	20·09						
9	15·703	12·8174	18·61	15·581	21·4	18·4						
	(17·20	11·34)										
	12·8176	15·7041	15·581	18·601	18·4	21·5						

TABLE 2. Calculated values of the complex coefficient, λ, in the fast-mode approximation (2) for $1 \leqslant n \leqslant 9$. The number of modes shown decreases for higher n because of decreasing accuracy. The accuracy of the coefficients, which also decreases for increasing $|\lambda|$, is indicated by the number of significant figures shown. The values in parentheses in the first column were calculated by Burridge (private communication).

		'Torsional' modes						'Meriodonal' modes					
BD		3·214	1·856	5·620	3·245	7·589	4·382	6·554	1·687	10·220	4·112	4·737	4·832
$\alpha = 10·0$	$n = 0$	3·214	1·856	5·620	3·244	7·591	4·380	6·552	1·677	10·177	3·945	4·737	4·844
	$n = 1$	3·214	1·856	5·619	3·246	7·586	4·384	6·557	1·665	10·173	3·929	4·732	4·862
	$n = 9$	3·213	1·856	5·593	3·221	7·597	4·398	6·589	1·600	10·273	3·866	4·694	4·917
$\alpha = 0·01$	$n = 0$	3·214	1·856	5·619	3·245	7·590	4·380	6·555	1·685	10·168	3·970	4·737	4·834
	$n = 1$	3·214	1·857	5·619	3·245	7·592	4·383	6·707	1·978	11·363	4·129	4·662	4·936
	$n = 9$	3·213	1·857	5·599	3·243	7·619	4·366	6·615	1·575	10·121	4·067	4·684	4·866

TABLE 3. Values of the complex coefficient, μ, in the slow-mode approximation (3). All of the imaginary parts are negative, but the negative signs have been omitted for clarity. BD denotes the values predicted by the approximation of Burridge & Drazin (1969). [See Antosiewicz (1970, p. 478) and Gill (1965) for tables of the zeros of the Airy function and zeros of the integral of the Airy function.] The numerical values for $\alpha = 10·0$ and $0·1$ and $n = 0, 1$ and 9 are an extrapolation to $\alpha R \rightarrow \infty$ based on a fit of (4) to our wave speed results for $\alpha R = 5 \times 10^4$, 1×10^5, and 2×10^5. The modes labelled 'torsional' are torsional modes for $n = 0$ and are related, in the theory of Burridge & Drazin, to zeros of the Airy function. The modes labelled 'meridional' are meridional for $n = 0$ and are related to zeros of the integral of the Airy function.

We wish to thank Mr William Torman who joined us in the latter stages of our research and spent many hours running most of our more recent results. This research could not have been carried out without the generous assistance of the SIT Computer Center and the ODU Computer Center.

REFERENCES

ANTOSIEWICZ, H. A. 1970 Bessel functions of fractional order. In *Handbook of Mathematical Functions* (ed. M. Abramowitz & I. A. Stegun). Washington: National Bureau of Standards.

BURRIDGE, D. M. & DRAZIN, P. G. 1969 *Phys. Fluids* **12**, 264–265.

COTTON, F. W. 1977 *A Study of the Linear Stability Problem for Viscous Incompressible Fluids in Circular Geometries by Means of a Matrix-Eigenvalue Approach.* Ph.D. dissertation, Stevens Institute of Technology. University Microfilms International, Ann Arbor, Mi. 48106 (Order no. 77-26, 931).

COTTON, F. W. & SALWEN, H. 1976 BESLIB (DECUS 10-272) and INDEX (DECUS 10-273). DEC Users Library, Maynard, Mass. 01754.

COTTON, F. W., SALWEN, H. & GROSCH, C. E. 1975 *Bull. Am. Phys. Soc.* **20**, 1416.

DI PRIMA, R. C. & HABETLER, G. J. 1969 *Arch. Rat. Mech.* **34**, 218–227.

GILL, A. E. 1965 *J. Fluid Mech.* **21**, 145–172.

LESSEN, M., SADLER, S. G. & LIU, T. Y. 1968 *Phys. Fluids* **11**, 1404–1409.

SALWEN, H. & GROSCH, C. E. 1972 *J. Fluid Mech.* **54**, 93–112.